Attenuation of influenza A virus disease severity by viral co-infection in a mouse model

Short Title: Pathogenesis of influenza viral co-infection

Andres J. Gonzalez, Emmanuel C. Ijezie, Onesmo B. Balemba, and Tanya A. Miura#

Department of Biological Sciences and Center for Modeling Complex Interactions, University of Idaho, Moscow, ID, USA

#Corresponding Author: Tanya A. Miura, tmiura@uidaho.edu

Abstract word count: 247

Text word count: 5,657

Abstract

Influenza viruses and rhinoviruses are responsible for a large number of acute respiratory viral infections in human populations and are detected as co-pathogens within hosts. Clinical and epidemiological studies suggest that co-infection by rhinovirus and influenza virus may reduce disease severity and that they may also interfere with each other's spread within a host population. To determine how co-infection by these two unrelated respiratory viruses affects pathogenesis, we established a mouse model using a minor serogroup rhinovirus (RV1B) and mouse-adapted influenza A virus (PR8). Infection of mice with RV1B two days before PR8 reduced pathogenesis of mild to moderate, but not severe PR8 infections. Disease attenuation was associated with an early inflammatory response in the lungs and enhanced clearance of PR8. However, co-infection by RV1B did not reduce PR8 viral loads early in infection or inhibit replication of PR8 within respiratory epithelia or *in vitro*. Inflammation in co-infected mice

remained focal, in comparison to diffuse inflammation and damage in the lungs of mice infected by PR8. These findings suggest that RV1B stimulates an early immune response that clears PR8 while limiting excessive pulmonary inflammation. The timing of RV1B co-infection was a critical determinant of protection, suggesting that sufficient time is needed to induce this response. Finally, disease attenuation was not unique to RV1B: co-infection by a murine coronavirus two days before PR8 also reduced disease severity. This model will be critical for understanding the mechanisms responsible for attenuation of influenza disease during co-infection by unrelated respiratory viruses.

Importance

Viral infections in the respiratory tract can cause severe disease and are responsible for a majority of pediatric hospitalizations. Molecular diagnostics have revealed that approximately 20% of these patients are infected by more than one unrelated viral pathogen. To understand how viral co-infection affects disease severity, we inoculated mice with a mild viral pathogen followed two days later by a virulent viral pathogen. This model demonstrated that rhinovirus can reduce the severity of influenza A virus, which corresponded with an early but controlled inflammatory response in the lungs and early clearance of influenza A virus. We further determined the dose and timing parameters that were important for effective disease attenuation and showed that influenza disease is also reduced by co-infection with a murine coronavirus. These findings demonstrate that co-infecting viruses can alter immune responses and pathogenesis in the respiratory tract.

Introduction

Respiratory tract infections are a leading cause of morbidity and mortality worldwide and viruses from many different families contribute to the disease burden. Advances in viral diagnostics and surveillance have led to the finding that viral co-infection, or the presence of multiple unrelated viruses, is quite common in the respiratory tract (1-3). Viruses involved in co-infections have the potential for interactions within the host that could affect replication dynamics, immune responses, and disease pathogenesis (4, 5).

Influenza viruses and rhinoviruses are common causes of both upper and lower respiratory tract infections across all age groups (6-8). Thus, it is not surprising that they are frequently detected in co-infected patients. During the 2009 pandemic, the severity of influenza was reduced by co-infection with rhinoviruses, though it was enhanced by co-infection with other respiratory viruses (9). These differences did not correspond with changes in viral replication, as equivalent H1N1 viral loads were detected in co-infected patients and those infected by influenza A virus alone (9). Other clinical studies have found that respiratory viral co-infection can enhance (10-12), reduce (13, 14), or have no effect (15) on the severity of influenza. These differences may be due to the viruses involved, the order that they infected the host, and differences in patient populations. The disease severity of rhinovirus infections has also been shown to be affected by viral co-infections. Co-infection by influenza viruses has been found to reduce the severity of rhinovirus infection (11) and co-infection by respiratory syncytial virus enhances disease compared to rhinovirus alone (11, 16-18). Finally, epidemiological studies suggest that rhinoviruses may interfere with the spread of influenza within populations (8, 19-22). Likewise, spread of the 2009 pandemic H1N1 strain appears to have delayed the circulation of other seasonal respiratory viruses (7). Altogether, these studies suggest that respiratory viruses have complex interactions at the host and population levels. Model systems in

which the viral strains and infection timing and doses are controlled are needed to understand these interactions at a mechanistic level.

In order to study the effects of viral co-infection on influenza disease pathogenesis, we established a mouse model of co-infection using mouse-adapted influenza A virus, strain PR8. PR8 infection in BALB/c mice causes dose-dependent disease severity, in which mortality corresponds with early viral replication and cytokine production, followed by massive cellular infiltration in the lungs (23-25). To determine how PR8-mediated disease is altered by a mild viral infection, we co-infected mice with human rhinovirus strain 1B (RV1B) or a murine coronavirus, mouse hepatitis virus (MHV-1). RV1B infects mice using low-density lipoprotein as its receptor, which is found on murine respiratory epithelial cells (26). Inoculation of BALB/c mice with an extremely high dose of RV1B results in neutrophil and lymphocyte recruitment to the airways, along with expression of antiviral and proinflammatory cytokines, without causing overt disease (27). MHV-1 is a respiratory tropic coronavirus that is a native pathogen of mice. While MHV-1 causes severe disease in A/J and TLR4-deficient mouse strains, it causes dose-dependent severity in the respiratory tract of BALB/c mice (28, 29).

Here, we show that RV1B (RV) reduced the pathogenesis of PR8 infection and that the severity of PR8 infection and the timing of co-infection were critical determinants of disease attenuation. Co-infection-mediated protection corresponded with early but controlled pulmonary inflammation and enhanced recovery of co-infected mice. RV1B did not prevent infection by PR8 or inhibit early replication, but led to faster clearance. Interestingly, attenuation of PR8 disease was not limited to co-infection by RV1B, it was also seen when mice were co-infected by MHV. By identifying the parameters that are critical for disease attenuation during co-infection, such as viral doses, order, and timing of infection, we have established a model system

in which we can determine how co-infecting viruses interact with the host's immune system to alter pathogenesis.

Results

RV infection two days before PR8 lessens disease severity in mice

Patients that are co-infected by H1N1 influenza A virus and rhinovirus have less severe disease than those that are co-infected by H1N1 and a non-rhinovirus (9). To evaluate the effects of rhinovirus co-infection on influenza disease severity, we inoculated mice with RV followed two days later by a low, medium, or high dose of PR8 ($PR8_{Low}$, $PR8_{Med,}$ or $PR8_{Hi}$). Control groups were inoculated with RV/mock or mock/PR8 on day -2/day 0. Mice were monitored daily for mortality and weight loss, and were given a score based on clinical signs of disease, including ruffled fur, hunched posture, lethargy, and labored breathing. Humane endpoints included loss of more than 25% of their starting weight and/or severe clinical signs of disease. Similar to previous studies (27), mice inoculated with RV had no mortality or morbidity, including weight loss and clinical signs (Fig. 1A, B, C; RV/Mock). Mice that were inoculated with RV had no distinguishable differences in weight loss or clinical signs from mice that received mock inoculations (data not shown). Mice inoculated with $PR8_{Low}$ (Mock/$PR8_{Low}$) reached 40% mortality by day 8, but the remaining mice survived until end of the study (Fig. 1A). These mice began losing weight and showing clinical signs on day 3, which progressed until the peak of disease on day 8 (Fig. 1B, C). Clinical signs of disease included minor ruffling of fur and hunching of the back, which progressed to include slightly labored breathing until eventual recovery from infection. In contrast to the mice infected with $PR8_{Low}$ alone, mice inoculated with

RV two days before $PR8_{Low}$ (RV/$PR8_{Low}$) all survived until the end of the study (Fig. 1A). Co-infected mice lost weight between days 3-7, but the rate of loss and maximum weight loss were less than mice infected by $PR8_{Low}$ alone (Fig. 1B). Clinical signs in co-infected mice were limited to minor ruffling and hunching and the onset of these signs was delayed until day 6 compared to mice infected with low dose PR8 alone (Fig. 1C).

RV-mediated disease attenuation was less effective when the dose of PR8 was increased. Mice that were inoculated with a medium dose of PR8 (Mock/$PR8_{Med}$) had increased mortality, weight loss, and clinical signs compared to Mock/$PR8_{Low}$. Furthermore, disease severity was only partially reduced by co-infection with RV (RV/$PR8_{Med}$). All mice inoculated with $PR8_{Med}$ alone succumbed to infection, whereas 2 of the 7 co-infected mice survived (Fig. 1D). Both groups of mice, Mock/$PR8_{Med}$ and RV/$PR8_{Med}$, began losing weight on day 3 and continued to day 8 (Fig. 1E). Mice inoculated with $PR8_{Med}$ alone had more severe clinical signs throughout PR8 infection, exhibited as severe ruffling, mild lethargy, hunching, and labored breathing (Fig. 1F). In contrast, co-infected (RV/$PR8_{Med}$) mice had milder clinical signs limited to mild ruffling, slight hunching, and lethargy, which resolved as the surviving mice began to regain weight.

RV did not alter disease severity when mice were infected with a high dose of PR8. All of the mice inoculated with a $PR8_{Hi}$ alone reached humane endpoints by day 7, one day earlier than mice inoculated with $PR8_{Med}$ (Fig. 1G vs. 1D). Mock/$PR8_{Hi}$-infected mice lost weight at a similar rate to mice to inoculated with Mock/$PR8_{Med}$ (Fig. 1H vs. 1E) but displayed more severe clinical signs at later times in infection (Fig. 1I vs. 1F). Mock/$PR8_{Hi}$-infected mice had moderate ruffling and hunching on day 3, which quickly progressed to severe ruffling and hunching and moderate-severe lethargy and labored breathing before succumbing to infection (Fig. 1I). Co-infected mice (RV/$PR8_{Hi}$) had no differences in mortality (Fig. 1G), weight loss (Fig. 1H), or

clinical signs (Fig. 1I) compared to mock/$PR8_{Hi}$-infected mice. In summary, RV lessened the severity of a mild or moderate, but not severe, infection by PR8 when inoculated two days before PR8.

Co-infection by RV leads to more rapid clearance of PR8 from the lungs

The above experiments established that RV effectively attenuated disease due to a mild PR8 infection. We next asked whether the reduced virulence during co-infection was due to inhibition of PR8 replication within the lungs. Groups of mice were either mock-inoculated or inoculated with RV two days before inoculating with a low dose of PR8 (Mock/PR8, RV/PR8). Groups of mice were euthanized on days 4, 7, and 10 after PR8 inoculation and lungs were harvested for PR8 quantification. On day 4 after PR8 inoculation, the viral loads in single virus and co-infected mice were not significantly different, but co-infected mice had greater variation within the group (Fig. 2). However, on day 7, the Mock/PR8-infected mice still had PR8 titers in the 10^4-10^5 range, whereas the RV/PR8-co-infected mice had undetectable levels of PR8. By day 10, both groups had undetectable levels of infectious PR8. This suggests that co-infection with RV did not prevent infection or inhibit early replication of PR8, but induced more rapid clearance of PR8 from the lungs.

We also evaluated lung sections for PR8 antigens by immunohistochemistry. The lack of PR8 antigen staining in lung sections from mock-inoculated mice confirmed the specificity of staining (Fig. 3A). On day 4, both single- and co-infected groups had extensive infection of the bronchial epithelium (not shown) in addition to viral antigen in bronchiolar epithelium and alveoli (Fig. 3B). The Mock/PR8-infected lung tissues had more extensive sloughing of infected

164 epithelia with viral antigens associated with mucopurulent material in the airways. While
165 Mock/PR8-infected animals had clear progression of infection from upper and lower airways
166 into the adjacent alveoli, co-infected animals appeared to have viral antigen in the alveoli earlier
167 and it was not always associated with infection of bronchiolar epithelium in the same region.
168 Both groups had extensive viral antigen staining in the alveoli, with antigen detected in
169 pneumocytes and immune cells, especially macrophages and neutrophils. On day 7, antigen
170 staining was reduced in lung tissues from both groups and was localized in airways, especially
171 cells that had been sloughed from the epithelium (Fig. 3C). PR8 antigens in the alveoli were
172 mainly found in immune cells by day 7, suggesting clearance of infection. In agreement with the
173 undetectable levels of infectious PR8, both groups had little antigen staining on day 10, which
174 was predominantly in immune cells within focal areas (not shown). These findings support our
175 observation that co-infection by RV did not completely inhibit replication of PR8 in the
176 respiratory tract.

177

178 **RV does not interfere with replication of PR8 *in vitro***

179 Next, we used a murine lung epithelial cell line (LA-4) that is susceptible to infection by
180 both viruses (30) to determine if co-infection by RV would interfere with PR8 replication *in vitro*.
181 LA-4 cells were inoculated with RV 6 or 12 hours before or simultaneously with PR8. PR8
182 released into the media was quantified by $TCID_{50}$ assay in MDCK cells. We confirmed that the
183 presence of RV in these samples did not interfere with quantification of PR8 in MDCK cells (not
184 shown). There were no significant differences at any time point between cells inoculated with
185 PR8 alone or co-infected with RV either simultaneously with or 12 hours before PR8 (Fig. 4A,
186 C). There were significant differences at 24 and 96 hours when cells were inoculated with RV 6

hours before PR8 (Fig. 4B). The lower PR8 titers at 96 hours may have been due to higher cell death from two viruses being present, providing fewer susceptible cells for PR8 replication. Though not significant, this trend was also seen when cells were inoculated with both viruses simultaneously (Fig. 4A). These data help corroborate our *in vivo* finding that RV did not inhibit replication of PR8. Rather, co-infection is most likely stimulating the immune system, leading to faster clearance of PR8.

Co-infection with RV stimulated an early yet controlled inflammatory response to PR8 infection

We next evaluated the histopathology of lungs from single- (Mock/PR8) and co- (RV/PR8) infected mice on days 4, 7, and 10 after inoculation with PR8. Compared to mock-inoculated controls, both Mock/PR8- and RV/PR8-infected mice had multifocal tracheobronchitis and bronchioalveolitis (Fig. 5 A-C and not shown). Lung pathology was characterized by epithelial degeneration, necrosis and sloughing, and accumulation of neutrophils, macrophages, and lymphocytes in the inflamed areas. This was associated with the accumulation of mucopurulent discharge in the bronchioles and alveoli (Fig. 5C). The extension of inflammation from bronchioles into the surrounding lung parenchyma resulted in localized alveolitis. In general, inflammation was associated with dilated and congested blood capillaries with extravasation of blood plasma, hemorrhage, thickened alveolar septae, collapsed alveoli, and enlarged alveolar ducts observed in severe lesions (Fig. 5B, C). Although focal inflammation was found in all lobes, the right lung's caval lobe appeared to be commonly more inflamed than other lobes. Pulmonary invagination was often associated with inflamed portions of the lungs.

Co-infection with RV induced earlier inflammation, but reduced the severity of inflammation elicited by PR8. By day 4, lung pathology was more extensive in RV/PR8 co-infected mice than Mock/PR8-infected mice. However, by days 7 and 10, mice infected with Mock/PR8 had more severe lung pathology than RV/PR8 co-infected mice. Overall, necrosis and desquamation in the trachea, bronchi, bronchioles, and alveoli were more severe in Mock/PR8 than in RV/PR8 co-infected mice. Furthermore, excessive mucopurulent material consisting of neutrophils, macrophages, cellular debris, and transudate accumulated in the lungs of Mock/PR8-infected mice. Congestion and hemorrhage were also more severe and pleurisy was only present in the lungs of Mock/PR8-infected mice. Furthermore, the expansion of bronchiolar inflammation into the parenchyma and collapse and destruction of alveoli was less extensive in lungs of RV/PR8 co-infected mice. Noteworthy, perivascular cuffing was more dense and widespread in RV/PR8 co-infected mice and their lungs had more lymphocytes and macrophages and fewer neutrophils than Mock/PR8-infected mice. These findings suggest that Mock/PR8-infected mice had more tissue damage and exacerbated inflammation while RV/PR8 co-infected mice had a more focused anti-viral cellular immune response.

Co-infection by RV also resulted in earlier resolution of inflammation and tissue regeneration. Type II pneumocyte hyperplasia and regeneration of the epithelium was observed in the bronchioles and alveoli of RV/PR8 co-infected mice on days 7 and 10, indicating signs of regeneration. Overall, there were fewer inflammatory cells in the alveoli in lungs of RV/PR8 co-infected mice compared with lungs of Mock/PR8-infected mice. Pleurisy was encountered in some of the lungs obtained from Mock/PR8-infected mice but not RV/PR8 co-infected mice. In summary, the findings of this study show that co-infecting mice with RV reduced the magnitude

of the inflammatory response to PR8 infection and accelerated epithelial repair and alveoli restoration, and the overall recovery.

The timing of RV co-infection determines the effect on disease severity during PR8 infection

Co-infection by RV was effective at reducing disease during a mild or moderate PR8 infection when given two days before PR8. We next determined whether co-infection with RV simultaneously with or two days after a low or medium dose of PR8 would also ameliorate disease. When RV and $PR8_{Low}$ were inoculated simultaneously (RV+$PR8_{Low}$), co-infection resulted in a disease phenotype intermediate between $PR8_{Low}$ alone (Mock/$PR8_{Low}$) and RV two days before $PR8_{Low}$ (RV/$PR8_{Low}$) (Fig. 6A-C). RV+$PR8_{Low}$ co-infected mice reached 33% mortality by day 9 (Fig. 6A). This mortality was higher than mice inoculated with RV two days before $PR8_{Low}$ (RV/$PR8_{Low}$), but significantly lower than the 100% mortality seen with mice infected with $PR8_{Low}$ alone (Mock/$PR8_{Low}$). RV+$PR8_{Low}$-infected mice lost weight at a similar rate to Mock/$PR8_{Low}$-infected mice, beginning on day 3 and continuing until day 8 before recovering (Fig. 6B). Average clinical scores were also similar between simultaneous co-infection and single infection, with slight lethargy, hunching, breathing, and moderate ruffling detected on day 3 and 4 and peaking with moderate lethargy, hunching, breathing, and severe ruffling on day 7 before co-infected mice (RV+$PR8_{Low}$) began recovering from infection (Fig. 6C). Interestingly, when RV was given two days after $PR8_{Low}$ ($PR8_{Low}$/RV), co-infection exacerbated PR8 disease, as evidenced by more rapid mortality, weight loss, and higher clinical scores than mice infected with Mock/$PR8_{Low}$ (Fig. 6A-C). $PR8_{Low}$/RV co-infected mice began dying and reached 100% mortality two days before mice inoculated with Mock/$PR8_{Low}$ (Fig. 6B).

$PR8_{Low}$/RV co-infected mice also lost weight at a greater rate and had dramatically higher clinical scores than other single virus- and co-infected groups (Fig. 6B, C). These increased clinical scores were due to severe lethargy and ruffling, moderate hunching, and labored breathing, which occurred earlier during infection compared to mice in the other groups (Fig. 6C).

In contrast to $PR8_{Low}$, RV was only effective at disease attenuation when given two days before a higher dose ($PR8_{Med}$) of PR8. There were no significant differences in mortality, weight loss, or clinical signs between simultaneously co-infected (RV+$PR8_{Med}$) mice and mice inoculated with $PR8_{Med}$ alone (Fig. 6D-F). Both of these groups steadily lost weight between days 3-8 and reached 100% mortality by day 8 (Fig. 6D, E). RV+$PR8_{Med}$ co-infected mice had slightly lower clinical scores than Mock/$PR8_{Med}$-infected mice (Fig. 6F), and did not experience severely labored breathing like Mock/$PR8_{Med}$-infected mice. However, these differences in clinical signs did not affect mortality. When RV was inoculated two days after $PR8_{Med}$ ($PR8_{Med}$/RV), all mice reached humane endpoints by day 7, one day earlier than mice inoculated with Mock/$PR8_{Med}$ (Fig. 6D). $PR8_{Med}$/RV co-infected mice lost weight at a similar rate to Mock/$PR8_{Med}$-infected mice and had similar clinical scores (Fig.6E-F). These data demonstrate that RV provides protection from PR8-induced disease in a time-dependent manner. Disease attenuation was most effective when RV had adequate time to activate a protective response.

Disease attenuation is not limited to co-infection by RV

We next evaluated whether attenuation of PR8 disease was limited to co-infection by RV or if a different respiratory virus would also be effective. Mice were either mock-inoculated or

inoculated with MHV two days before PR8 and monitored for survival and weight loss over 14 days. One mouse inoculated with $2x10^3$ PFU of MHV (MHV_{2000}/Mock) reached a humane endpoint, but the remaining mice survived until the end of the study (Fig. 7A). MHV-infected mice (MHV_{2000}/Mock) had rapid, early weight loss followed by gradual recovery of weight (Fig. 7B). These mice had moderate ruffling and hunching early in infection, which reduced to slight ruffling, lethargy, and hunching before finally recovering on day 13 (Fig. 7C). Despite the prolonged morbidity in MHV-infected mice, mice co-infected with a lethal dose of PR8 (MHV_{2000}/PR8) had similar mortality and morbidity as those infected by MHV alone (Fig. 7A-C). MHV_{2000}/PR8 co-infected mice regained weight at a slower rate than mice inoculated with MHV_{2000}/Mock, but eventually reached the same weight (Fig. 7B). Thus, co-infection by MHV reduced the severity of PR8-induced disease, but this dose of MHV caused significant morbidity in BALB/c mice.

To determine whether infection by a lower dose of MHV would cause less disease but still provide protection against PR8, we tested two additional doses of MHV: $1x10^3$ PFU (MHV_{1000}) and $2x10^2$ PFU (MHV_{200}). When mice were inoculated with the 2-fold lower dose of MHV (MHV_{1000}/Mock), there was no mortality associated with infection (Fig. 7D). These mice lost weight very early in infection, but did not lose as much weight as those infected by the higher dose (Fig. 7E vs. B). MHV_{1000}/Mock-infected mice had minor ruffling and hunching on day 0, which continued until day 9 (Fig. 7F). When MHV was inoculated two days before PR8 (MHV_{1000}/PR8), only one mouse reached a humane endpoint, and mortality was delayed until day 8, compared to day 5 for the higher dose of MHV (Fig. 7D vs. A). Similar to mice infected by MHV_{1000} alone, MHV_{1000}/PR8 co-infected mice lost weight early. However, co-infected mice had delayed recovery of weight and their weight was still lower than MHV_{1000}-infected mice at

the end of the study (Fig. 7E), which corresponded with prolonged clinical signs of disease (Fig. 7F). Although this lower dose of MHV caused a milder infection and provided similar protection against PR8-mediated mortality, morbidity was prolonged in the co-infected mice suggesting it was less effective than the higher dose.

When mice were inoculated with a 10-fold lower dose of MHV (MHV_{200}/Mock), they all survived and had minimal weight loss and clinical signs of disease, which was limited to slight ruffling (Fig. 7G-I). However, mice that were co-infected with this low dose of MHV prior to PR8 (MHV_{200}/PR8) had significant mortality, weight loss, and prolonged clinical signs of disease, including moderate lethargy and labored breathing (Fig. 6G-I). Even though this lowest dose of MHV caused minimal disease in BALB/c mice, it did not protect mice against PR8-induced morbidity and mortality. These data suggest that a dose of MHV that causes significant morbidity is required to effectively protect against a lethal dose of PR8. Although both RV and MHV given two days earlier both reduced the severity of PR8, they vary in pathogenesis and effectiveness of disease attenuation.

Discussion

Clinical studies have suggested that respiratory viral co-infections may alter pathogenesis compared to infection by the viruses individually. RV has been implicated in both interfering with the spread of influenza viruses and reducing the severity of influenza during co-infection (8, 9, 19-22). Here, we developed a murine model of respiratory viral co-infection to study the effects on disease severity in a system where we can control the virus strains, doses, order, and timing of which they infect the host. We found that mice given RV two days before PR8 were

completely protected against mortality and had reduced morbidity. RV was less effective at disease attenuation when mice were given higher doses of PR8, or RV was given at the same time as PR8. Further, mice given RV two days after PR8 had enhanced disease compared to PR8 alone. We also found that disease attenuation was not limited to co-infection by RV. A respiratory tropic strain of MHV also reduced PR8 disease when given two days before PR8. Unlike RV, MHV caused significant morbidity in mice. However, reducing the dose of MHV to lessen pathogenesis was less effective at reducing the severity of PR8. These data suggest that changes in pathogenesis during co-infection are dependent upon the severity of each infection and the order and timing of inoculation.

Despite preventing mortality and significantly inhibiting morbidity, infection of mice with RV two days before PR8 did not reduce PR8 levels in the lungs early in infection (Fig. 2) or prevent spread of PR8 within the respiratory tract (Fig. 3). These findings suggest that RV does not directly inhibit infection by PR8, which was also confirmed by our *in vitro* studies (Fig. 4). Our previous studies have shown that RV induces a robust type I IFN response in the LA-4 cell line (30), thus the lack of PR8 inhibition we saw is not due to the absence of an IFN response. This is not surprising, as the NS1 protein of PR8 is known to antagonize type I IFN responses (31). Others have shown that RV induces expression of type I and type III IFNs in the respiratory tract of infected mice (27, 32, 33). Although our data do not support a role for RV-induced IFN responses in preventing infection by PR8, IFNs may be important for inducing downstream antiviral responses that contribute to earlier clearance of PR8 in co-infected animals. In addition to promoting cell-intrinsic antiviral defense strategies, type I IFNs are important for the recruitment and functional phenotypes of myeloid cell responses to influenza virus infections (34, 35). In the absence of type I IFN signaling, PR8 disease severity is increased, but the enhanced

disease is not completely due to increased viral loads. Rather, these studies showed that type I IFN signaling is needed to down-regulate inflammatory monocyte and neutrophil responses during PR8 infection. Furthermore, in the absence of type I IFN signaling, monocytes develop increased inflammatory phenotypes and reduced expression of genes that down-regulate inflammation (34, 35). Thus, type I IFN responses induced by RV could promote down-regulation of inflammation that we observed on days 7 and 10.

Histopathology analyses demonstrated that mice inoculated with RV two days before PR8 had earlier recruitment of immune cells into the lungs (Fig. 5). On day 4 after PR8 infection, co-infected animals had multiple foci of inflammation throughout the lungs. In contrast, animals infected with PR8 alone had reduced recruitment of inflammatory cells. This early immune response may lead to earlier clearance of PR8 from co-infected lungs, as we saw by day 7 (Fig. 2). Although it is not virulent in mice, RV (strain 1B) induces an inflammatory response in the respiratory tracts of BALB/c and C57Bl/6 mice. The response to RV includes recruitment of neutrophils and lymphocytes, concurrent with production of antiviral cytokines and chemokines. Neutrophil levels in the airways of RV-infected mice peak on days 1 and 2 and decline by day 4, while lymphocytes are present through day 7 (27, 32, 33, 36, 37). Studies differ in whether macrophage numbers change significantly upon RV infection in mice (27, 32, 33, 36). Type I and III interferons, proinflammatory cytokines, and neutrophil and lymphocyte recruiting chemokines are also up-regulated in response to RV infection in mice (27, 32, 33). These cellular and cytokine responses are not stimulated by UV-inactivated virus, suggesting that viral replication is required (27, 33). We observed increased macrophages and lymphocytes and enhanced perivascular cuffing in histology sections from RV/PR8 co-infected animals,

366 suggesting a robust cellular immune response. Ongoing studies in our lab will determine the RV-
367 induced immune components that are required for attenuation of PR8 disease during co-infection.

368 In contrast to the enhanced inflammation in the lungs of co-infected mice on day 4, the
369 histopathology on days 7 and 10 was less severe in co-infected compared to PR8-infected mice
370 (Fig. 5). This could be an indirect consequence of early viral clearance (Fig. 2) or active down-
371 regulation of the inflammatory response in co-infected animals. Multiple studies have shown that
372 inflammation during influenza and other respiratory viral infections can cause pathogenesis that
373 is independent of viral levels in the lungs (34, 35, 38-40). Our histopathology data are in
374 agreement with studies that demonstrate excessive inflammatory responses occurring as viral
375 loads are decreasing (23, 41). We inoculated mice with PR8 two days after RV inoculation,
376 which is just prior to the decline in neutrophil numbers in the lungs of RV-infected BALB/c mice
377 (27). Furthermore, RV infection actively down-regulates neutrophil responses by inhibiting TLR
378 signaling and thereby reducing expression of neutrophil-specific chemokines upon co-infection
379 by a bacterial pathogen (42). The inflamed areas of the RV/PR8 co-infected lungs contained
380 fewer neutrophils than mock/PR8-infected lungs. Neutrophils are known to contribute to
381 immune-mediated damage during PR8 infection (43, 44). Thus, active down-regulation of
382 neutrophilic inflammation by RV may contribute to the reduced severity of PR8 in our studies.

383 This study demonstrated that RV-mediated disease attenuation was less effective as we
384 increased the dose of PR8, shortened the timing between virus inoculations, or gave RV after
385 PR8 (Figs. 1 and 6). These differences are likely due to the kinetics and magnitudes of RV- and
386 PR8-induced immune responses. Higher doses of PR8 likely overwhelm defense mechanisms
387 that are induced by RV and these defense mechanisms are likely not induced quickly enough to
388 completely protect against PR8 given at the same time. However, the observation that RV given

two days after PR8 exacerbates pathogenesis suggests that once a response to PR8 has been initiated, the RV-induced response may aggravate immunopathology. RV induces multiple immune components that are known to contribute to influenza disease, including neutrophils (43), NK cells (45), and type I IFNs (46, 47). Further studies are needed to identify the mechanisms that exacerbate disease when RV is given 2 days after PR8. It is possible that these are the same mechanisms that reduce disease when RV is given 2 days before PR8 and that the timing of their induction is key to regulating pathogenesis.

Interestingly, infection by MHV two days prior to PR8 also reduced the severity of PR8 infection. Unlike RV, MHV causes morbidity and mortality in mice, though virulence is mouse strain-dependent (28, 29, 48). We have observed dose-dependent severity of MHV in BALB/c mice. Intranasal inoculation of 2×10^3 PFU resulted in clinical disease with low mortality (Fig. 7), while a dose of 2×10^5 caused 100% mortality (data not shown). Survival of BALB/c mice upon MHV-1 infection is dependent upon a type I IFN response (49). Furthermore, mouse strain-dependent resistance to MHV-1 disease corresponds with robust expression of type I IFNs (28). Based on these studies, we expect that the type I IFN response is adequate to protect BALB/c from a lower dose, but not a lethal dose, of MHV. Other components of the BALB/c immune response to MHV-1 infection have not been studied in detail. A complete understanding of this response will be important in determining the similarities and differences in the mechanisms whereby MHV and RV reduce the severity of PR8.

Although our viral inoculations were all within two days of each other, other studies have shown that infection of mice by one virus can alter the immune response to a heterologous virus given after resolution of the initial infection (50). Mice given lymphocytic choriomeningitis virus (LCMV), murine cytomegalovirus (MCMV), or PR8 six weeks prior to vaccinia virus had

412 reduced titers of vaccinia virus compared to control mice. However, infection with PR8 six
413 weeks prior to LCMV or MCMV increased titers of the second virus. Protection was associated
414 with changing from a response dominated by neutrophils to lymphocytes or a Th2 response to a
415 Th1 response. In contrast, when pigs were infected with porcine reproductive and respiratory
416 syndrome virus they had increased severity of porcine respiratory coronavirus infection, which
417 corresponded with an increased Th1 cytokine response and reduced NK cell and type I IFN
418 responses (51). Characterizing the immune responses across our various co-infection pairs and
419 infection timings will provide insight into how different viruses mediate heterologous immunity
420 and if these mechanisms are generalizable.

421

422 ## Materials and Methods

423

424 ### Virus stocks and cell lines

425 Madin-Darby canine kidney cells (MDCK; ATCC #CCL-34), murine fibroblast line 17Cl.1 (52)
426 (provided by Dr. Kathryn Holmes, University of Colorado Denver School of Medicine), and
427 HeLa cells (ATCC #CCL-2) were grown in Dulbecco's modified Eagle medium (DMEM)
428 supplemented with 10% fetal bovine serum (FBS; Atlanta Biologicals), and 1X antibiotic-
429 antimycotic (ThermoFisher). Murine lung epithelial cells (LA-4; ATCC #CL-196) were grown in
430 Ham's F12 (Kaign's modified) media (F12K; Caisson) supplemented with 10-15% FBS and
431 antibiotics. PR8 (A/Puerto Rico/8/1934 (H1N1)), obtained from BEI Resources (NR-3169), was
432 grown and titrated by tissue culture infectious dose-50% ($TCID_{50}$) assay in MDCK cells. MHV-1
433 (ATCC #VR-261) was grown and titrated by plaque assay in 17Cl.1 cells. RV1B (ATCC #VR-

1645) was grown and titrated by $TCID_{50}$ assay in HeLa cells. RV1B stocks were concentrated by centrifugation through 30% sucrose and the virus pellet was resuspended in PBS/2% FBS.

Mouse infections

All experimental protocols were approved by the University of Idaho Institutional Animal Care and Use Committee, following the National Institutes of Health Guide for the Care and Use of Laboratory Animals. As described below, mice were monitored daily and were euthanized by an overdose of sodium pentobarbital if they reached humane endpoints.

Six to eight-week-old female BALB/c mice were purchased from Harlan Laboratories/Envigo. Mice were housed in individually vented cages with controlled light/dark cycles and regulated temperature maintained by University of Idaho Lab Animal Research Facilities and received food and water *ad libitum*. Mice were acclimatized to the facility for 5-12 days before experiments were performed under ABSL2 conditions. Mice were anesthetized with inhaled isoflurane and inoculated intranasally with 50 uL of virus. For co-infections, mice were inoculated with each virus 2 days apart or simultaneously in a total 50 uL volume. Control mice received mock inoculations of the same buffer as the respective virus: RV (PBS/2% FBS), PR8 (MEM/2% FBS) or MHV (DMEM/10%FBS). See the results sections and figure legends for viral doses used in each experiment.

Mice were weighed and observed for clinical signs of disease daily and were humanely euthanized if they lost more than 25% of their starting weight or exhibited severe clinical signs of disease. Mice were given a daily severity score of 0-3 in each of four categories: ruffled fur,

455 lethargy, labored breathing, and hunched posture. The daily scores were totaled for each
456 individual mice and averaged across the group of mice.

457

458 **PR8 quantification**

459 Right lobes of the lungs were flash-frozen and stored at -80°C. Frozen tissues were weighed and
460 homogenized in DMEM with 2% BSA and 1% antibiotics, and PR8 was quantified by $TCID_{50}$
461 assay on MDCK cells (53). RV does not interfere with titration of PR8 in co-infected samples
462 when using the MDCK cell line (data not shown).

463

464 **Histology and immunohistochemistry**

465 The tracheas of euthanized mice were cannulated, and the lungs were inflated with 10% formalin
466 before submerging in 10% formalin. After fixation, lungs were embedded in paraffin, cut in 5 um
467 sections, and stained with modified Harris hematoxylin and eosin (VWR Scientific). Lungs were
468 processed for immunohistochemistry in the same manner as for histology. Tissue sections were
469 deparaffinized, rehydrated, and subjected to heat-induced antigen retrieval in 10 mM sodium
470 citrate buffer (pH 6) with 0.01% Tween 20. Endogenous peroxidase and alkaline phosphatase
471 activities were inhibited with BLOXALL solution (Vector Laboratories). Lung sections were
472 immunostained for the PR8 hemagglutinin protein (HA) using a polyclonal goat antibody (NR-
473 3148, BEI Resources) and an alkaline phosphatase conjugated anti-goat antibody (ImmPRESS,
474 Vector Laboratories) with detection by ImmPACT Vector Red (Vector Laboratories) and
475 counterstaining with hematoxylin. Images were acquired with a Zeiss Axio Lab.A1 microscope
476 with an Axiocam 105 color camera using ZEN 2.3 software (Zeiss).

In vitro co-infection experiments

LA-4 cells were inoculated with PR8 (MOI=1) either 6 or 12 h after or simultaneously with inoculation with RV (MOI=1). After 1 h incubation with the inoculum, cells were washed twice with serum-free medium, then incubated in Ham's F12K medium with 2% FBS and antibiotics at 37°C. Supernatant media was collected from the cells at 6, 12, 18, 24, 48, 72, and 96 hours after PR8 inoculation and PR8 was titrated by $TCID_{50}$ assay using MDCK cells.

Statistics

Statistical analyses were performed using Graphpad Prism 6 software. Survival curves were compared using log-rank Mantel-Cox curve comparison. Weight loss and clinical score data were compared using multiple student's *t* tests with Holm-Sidak multiple comparison correction. PR8 titers from mouse lungs and cell culture experiments were compared using student's *t* tests without correction for multiple comparisons.

Acknowledgements

Research reported in this publication was supported by the National Institute of General Medical Sciences of the National Institutes of Health under Award Number P20GM104420. The content is solely the responsibility of the authors and does not necessarily represent the official views of the National Institutes of Health. The following reagents were obtained through the NIH Biodefense and Emerging Infections Research Resources Repository, NIAID, NIH: Influenza A

Virus, A/Puerto Rico/8/34 (H1N1) and Polyclonal Anti-Influenza Virus H1 (H0) Hemagglutinin (HA), A/Puerto Rico/8/34 (H1N1) Antiserum, Goat (NR-3148). The authors would like to thank Mr. John Clary, Dr. Bhim Thapa, Ms. Jade Rodgers, and Ms. Alicia Healey for excellent technical support. We are also grateful to Dr. George Hodges for providing critical review of the pathology and manuscript.

References

1. **Brunstein JD, Cline CL, McKinney S, Thomas E.** 2008. Evidence from multiplex molecular assays for complex multipathogen interactions in acute respiratory infections. J Clin Microbiol **46:**97-102.
2. **Fairchok MP, Martin ET, Chambers S, Kuypers J, Behrens M, Braun LE, Englund JA.** 2010. Epidemiology of viral respiratory tract infections in a prospective cohort of infants and toddlers attending daycare. J Clin Virol **49:**16-20.
3. **Calvo C, Garcia-Garcia ML, Blanco C, Vazquez MC, Frias ME, Perez-Brena P, Casas I.** 2008. Multiple simultaneous viral infections in infants with acute respiratory tract infections in Spain. J Clin Virol **42:**268-272.
4. **DaPalma T, Doonan BP, Trager NM, Kasman LM.** 2010. A systematic approach to virus-virus interactions. Virus Res **149:**1-9.
5. **Opatowski L, Baguelin M, Eggo RM.** 2018. Influenza interaction with cocirculating pathogens and its impact on surveillance, pathogenesis, and epidemic profile: A key role for mathematical modelling. PLoS Pathog **14:**e1006770.
6. **Jain S, Williams DJ, Arnold SR, Ampofo K, Bramley AM, Reed C, Stockmann C, Anderson EJ, Grijalva CG, Self WH, Zhu Y, Patel A, Hymas W, Chappell JD, Kaufman RA, Kan JH, Dansie D, Lenny N, Hillyard DR, Haynes LM, Levine M, Lindstrom S, Winchell JM, Katz JM, Erdman D, Schneider E, Hicks LA, Wunderink RG, Edwards KM, Pavia AT, McCullers JA, Finelli L, Team CES.** 2015. Community-acquired pneumonia requiring hospitalization among U.S. children. N Engl J Med **372:**835-845.
7. **Grondahl B, Ankermann T, von Bismarck P, Rockahr S, Kowalzik F, Gehring S, Meyer C, Knuf M, Puppe W.** 2014. The 2009 pandemic influenza A(H1N1) coincides with changes in the epidemiology of other viral pathogens causing acute respiratory tract infections in children. Infection **42:**303-308.
8. **Greer RM, McErlean P, Arden KE, Faux CE, Nitsche A, Lambert SB, Nissen MD, Sloots TP, Mackay IM.** 2009. Do rhinoviruses reduce the probability of viral co-detection during acute respiratory tract infections? J Clin Virol **45:**10-15.
9. **Esper FP, Spahlinger T, Zhou L.** 2011. Rate and influence of respiratory virus co-infection on pandemic (H1N1) influenza disease. J Infect **63:**260-266.

10. **Papadopoulos NG, Moustaki M, Tsolia M, Bossios A, Astra E, Prezerakou A, Gourgiotis D, Kafetzis D.** 2002. Association of rhinovirus infection with increased disease severity in acute bronchiolitis. Am J Respir Crit Care Med **165:**1285-1289.
11. **Aberle JH, Aberle SW, Pracher E, Hutter HP, Kundi M, Popow-Kraupp T.** 2005. Single versus dual respiratory virus infections in hospitalized infants: impact on clinical course of disease and interferon-gamma response. Pediatr Infect Dis J **24:**605-610.
12. **Marcos MA, Ramon S, Anton A, Martinez E, Vilella A, Olive V, Cilloniz C, Moreno A, Torres A, Pumarola T.** 2011. Clinical relevance of mixed respiratory viral infections in adults with influenza A H1N1. Eur Respir J **38:**739-742.
13. **Martin ET, Kuypers J, Wald A, Englund JA.** 2012. Multiple versus single virus respiratory infections: viral load and clinical disease severity in hospitalized children. Influenza Other Respi Viruses **6:**71-77.
14. **Martinez-Roig A, Salvado M, Caballero-Rabasco MA, Sanchez-Buenavida A, Lopez-Segura N, Bonet-Alcaina M.** 2015. Viral coinfection in childhood respiratory tract infections. Arch Bronconeumol **51:**5-9.
15. **Camargo C, Guatura SB, Bellei N.** 2012. Respiratory viral coinfection among hospitalized patients with H1N1 2009 during the first pandemic wave in Brazil. Braz J Infect Dis **16:**180-183.
16. **Yoshida LM, Suzuki M, Nguyen HA, Le MN, Dinh Vu T, Yoshino H, Schmidt WP, Nguyen TT, Le HT, Morimoto K, Moriuchi H, Dang DA, Ariyoshi K.** 2013. Respiratory syncytial virus: co-infection and paediatric lower respiratory tract infections. Eur Respir J **42:**461-469.
17. **Marguet C, Lubrano M, Gueudin M, Le Roux P, Deschildre A, Forget C, Couderc L, Siret D, Donnou MD, Bubenheim M, Vabret A, Freymuth F.** 2009. In very young infants severity of acute bronchiolitis depends on carried viruses. PLoS One **4:**e4596.
18. **Richard N, Komurian-Pradel F, Javouhey E, Perret M, Rajoharison A, Bagnaud A, Billaud G, Vernet G, Lina B, Floret D, Paranhos-Baccala G.** 2008. The impact of dual viral infection in infants admitted to a pediatric intensive care unit associated with severe bronchiolitis. Pediatric Infectious Disease Journal **27:**213-217.
19. **Anestad G, Nordbo SA.** 2011. Virus interference. Did rhinoviruses activity hamper the progress of the 2009 influenza A (H1N1) pandemic in Norway? Med Hypotheses **77:**1132-1134.
20. **Casalegno JS, Ottmann M, Duchamp MB, Escuret V, Billaud G, Frobert E, Morfin F, Lina B.** 2010. Rhinoviruses delayed the circulation of the pandemic influenza A (H1N1) 2009 virus in France. Clin Microbiol Infect **16:**326-329.
21. **Linde A, Rotzen-Ostlund M, Zweygberg-Wirgart B, Rubinova S, Brytting M.** 2009. Does viral interference affect spread of influenza? Euro Surveill **14**.
22. **Pascalis H, Temmam S, Turpin M, Rollot O, Flahault A, Carrat F, de Lamballerie X, Gerardin P, Dellagi K.** 2012. Intense co-circulation of non-influenza respiratory viruses during the first wave of pandemic influenza pH1N1/2009: a cohort study in Reunion Island. PLoS One **7:**e44755.
23. **Vogel AJ, Harris S, Marsteller N, Condon SA, Brown DM.** 2014. Early cytokine dysregulation and viral replication are associated with mortality during lethal influenza infection. Viral Immunol **27:**214-224.

24. **Fukushi M, Ito T, Oka T, Kitazawa T, Miyoshi-Akiyama T, Kirikae T, Yamashita M, Kudo K.** 2011. Serial histopathological examination of the lungs of mice infected with influenza A virus PR8 strain. PLoS One **6:**e21207.

25. **Sugamata R, Dobashi H, Nagao T, Yamamoto K, Nakajima N, Sato Y, Aratani Y, Oshima M, Sata T, Kobayashi K, Kawachi S, Nakayama T, Suzuki K.** 2012. Contribution of neutrophil-derived myeloperoxidase in the early phase of fulminant acute respiratory distress syndrome induced by influenza virus infection. Microbiol Immunol **56:**171-182.

26. **Tuthill TJ, Papadopoulos NG, Jourdan P, Challinor LJ, Sharp NA, Plumpton C, Shah K, Barnard S, Dash L, Burnet J, Killington RA, Rowlands DJ, Clarke NJ, Blair ED, Johnston SL.** 2003. Mouse respiratory epithelial cells support efficient replication of human rhinovirus. J Gen Virol **84:**2829-2836.

27. **Bartlett NW, Walton RP, Edwards MR, Aniscenko J, Caramori G, Zhu J, Glanville N, Choy KJ, Jourdan P, Burnet J, Tuthill TJ, Pedrick MS, Hurle MJ, Plumpton C, Sharp NA, Bussell JN, Swallow DM, Schwarze J, Guy B, Almond JW, Jeffery PK, Lloyd CM, Papi A, Killington RA, Rowlands DJ, Blair ED, Clarke NJ, Johnston SL.** 2008. Mouse models of rhinovirus-induced disease and exacerbation of allergic airway inflammation. Nat Med **14:**199-204.

28. **De Albuquerque N, Baig E, Ma X, Zhang J, He W, Rowe A, Habal M, Liu M, Shalev I, Downey GP, Gorczynski R, Butany J, Leibowitz J, Weiss SR, McGilvray ID, Phillips MJ, Fish EN, Levy GA.** 2006. Murine hepatitis virus strain 1 produces a clinically relevant model of severe acute respiratory syndrome in A/J mice. J Virol **80:**10382-10394.

29. **Khanolkar A, Hartwig SM, Haag BA, Meyerholz DK, Harty JT, Varga SM.** 2009. Toll-like receptor 4 deficiency increases disease and mortality after mouse hepatitis virus type 1 infection of susceptible C3H mice. J Virol **83:**8946-8956.

30. **VanLeuven JT, Ridenhour BJ, Gonzalez AJ, Miller CR, Miura TA.** 2017. Lung epithelial cells have virus-specific and shared gene expression responses to infection by diverse respiratory viruses. PLoS One **12:**e0178408.

31. **Garcia-Sastre A, Egorov A, Matassov D, Brandt S, Levy DE, Durbin JE, Palese P, Muster T.** 1998. Influenza A virus lacking the NS1 gene replicates in interferon-deficient systems. Virology **252:**324-330.

32. **Glanville N, Peel TJ, Schroder A, Aniscenko J, Walton RP, Finotto S, Johnston SL.** 2016. Tbet Deficiency Causes T Helper Cell Dependent Airways Eosinophilia and Mucus Hypersecretion in Response to Rhinovirus Infection. PLoS Pathog **12:**e1005913.

33. **Girkin J, Hatchwell L, Foster P, Johnston SL, Bartlett N, Collison A, Mattes J.** 2015. CCL7 and IRF-7 Mediate Hallmark Inflammatory and IFN Responses following Rhinovirus 1B Infection. J Immunol **194:**4924-4930.

34. **Seo SU, Kwon HJ, Ko HJ, Byun YH, Seong BL, Uematsu S, Akira S, Kweon MN.** 2011. Type I interferon signaling regulates Ly6C(hi) monocytes and neutrophils during acute viral pneumonia in mice. PLoS Pathog **7:**e1001304.

35. **Stifter SA, Bhattacharyya N, Pillay R, Florido M, Triccas JA, Britton WJ, Feng CG.** 2016. Functional Interplay between Type I and II Interferons Is Essential to Limit Influenza A Virus-Induced Tissue Inflammation. PLoS Pathog **12:**e1005378.

36. **Chung Y, Hong JY, Lei J, Chen Q, Bentley JK, Hershenson MB.** 2015. Rhinovirus infection induces interleukin-13 production from CD11b-positive, M2-polarized exudative macrophages. Am J Respir Cell Mol Biol **52:**205-216.

37. **Ganesan S, Pham D, Jing Y, Farazuddin M, Hudy MH, Unger B, Comstock AT, Proud D, Lauring AS, Sajjan US.** 2016. TLR2 Activation Limits Rhinovirus-Stimulated CXCL-10 by Attenuating IRAK-1-Dependent IL-33 Receptor Signaling in Human Bronchial Epithelial Cells. J Immunol **197:**2409-2420.

38. **Oshansky CM, Gartland AJ, Wong SS, Jeevan T, Wang D, Roddam PL, Caniza MA, Hertz T, Devincenzo JP, Webby RJ, Thomas PG.** 2014. Mucosal immune responses predict clinical outcomes during influenza infection independently of age and viral load. Am J Respir Crit Care Med **189:**449-462.

39. **Rutigliano JA, Sharma S, Morris MY, Oguin TH, 3rd, McClaren JL, Doherty PC, Thomas PG.** 2014. Highly pathological influenza A virus infection is associated with augmented expression of PD-1 by functionally compromised virus-specific CD8+ T cells. J Virol **88:**1636-1651.

40. **Lin KL, Suzuki Y, Nakano H, Ramsburg E, Gunn MD.** 2008. CCR2+ monocyte-derived dendritic cells and exudate macrophages produce influenza-induced pulmonary immune pathology and mortality. J Immunol **180:**2562-2572.

41. **Le Goffic R, Balloy V, Lagranderie M, Alexopoulou L, Escriou N, Flavell R, Chignard M, Si-Tahar M.** 2006. Detrimental contribution of the Toll-like receptor (TLR)3 to influenza A virus-induced acute pneumonia. PLoS Pathog **2:**e53.

42. **Unger BL, Faris AN, Ganesan S, Comstock AT, Hershenson MB, Sajjan US.** 2012. Rhinovirus attenuates non-typeable Hemophilus influenzae-stimulated IL-8 responses via TLR2-dependent degradation of IRAK-1. PLoS Pathog **8:**e1002969.

43. **Narasaraju T, Yang E, Samy RP, Ng HH, Poh WP, Liew AA, Phoon MC, van Rooijen N, Chow VT.** 2011. Excessive neutrophils and neutrophil extracellular traps contribute to acute lung injury of influenza pneumonitis. Am J Pathol **179:**199-210.

44. **Ichikawa A, Kuba K, Morita M, Chida S, Tezuka H, Hara H, Sasaki T, Ohteki T, Ranieri VM, dos Santos CC, Kawaoka Y, Akira S, Luster AD, Lu B, Penninger JM, Uhlig S, Slutsky AS, Imai Y.** 2013. CXCL10-CXCR3 enhances the development of neutrophil-mediated fulminant lung injury of viral and nonviral origin. Am J Respir Crit Care Med **187:**65-77.

45. **Zhou G, Juang SW, Kane KP.** 2013. NK cells exacerbate the pathology of influenza virus infection in mice. Eur J Immunol **43:**929-938.

46. **Marois I, Cloutier A, Garneau E, Richter MV.** 2012. Initial infectious dose dictates the innate, adaptive, and memory responses to influenza in the respiratory tract. J Leukoc Biol **92:**107-121.

47. **Davidson S, Crotta S, McCabe TM, Wack A.** 2014. Pathogenic potential of interferon alphabeta in acute influenza infection. Nat Commun **5:**3864.

48. **Khanolkar A, Hartwig SM, Haag BA, Meyerholz DK, Epping LL, Haring JS, Varga SM, Harty JT.** 2009. Protective and pathologic roles of the immune response to mouse hepatitis virus type 1: implications for severe acute respiratory syndrome. J Virol **83:**9258-9272.

49. **Channappanavar R, Fehr AR, Vijay R, Mack M, Zhao J, Meyerholz DK, Perlman S.** 2016. Dysregulated Type I Interferon and Inflammatory Monocyte-Macrophage

Responses Cause Lethal Pneumonia in SARS-CoV-Infected Mice. Cell Host Microbe **19:**181-193.

50. **Chen HD, Fraire AE, Joris I, Welsh RM, Selin LK.** 2003. Specific history of heterologous virus infections determines anti-viral immunity and immunopathology in the lung. Am J Pathol **163:**1341-1355.

51. **Jung K, Renukaradhya GJ, Alekseev KP, Fang Y, Tang Y, Saif LJ.** 2009. Porcine reproductive and respiratory syndrome virus modifies innate immunity and alters disease outcome in pigs subsequently infected with porcine respiratory coronavirus: implications for respiratory viral co-infections. J Gen Virol **90:**2713-2723.

52. **Sturman LS, Takemoto KK.** 1972. Enhanced growth of a murine coronavirus in transformed mouse cells. Infect Immun **6:**501-507.

53. **Szretter KJ, Balish AL, Katz JM.** 2006. Influenza: propagation, quantification, and storage. Curr Protoc Microbiol **Chapter 15:**Unit 15G 11.

Figure Legends

FIG 1 Disease kinetics in mice infected by PR8 or co-infected with RV two days before PR8. Mice were either mock-inoculated or inoculated with $7.6x10^6$ $TCID_{50}$ units of RV on day -2. On day 0, mice were either mock-inoculated or inoculated with PR8 at (A-C) ~100 ($PR8_{Low}$), (D-F) ~200 ($PR8_{Med}$), or (G-I) ~$7.5x10^3$ ($PR8_{Hi}$) $TCID_{50}$ units. Mice were monitored for (A, D, G) mortality, (B, E, H) weight loss, and (C, F, I) clinical signs of disease, including lethargy, ruffled fur, hunched back, and labored breathing. Clinical scores were assigned on a scale of 0-3 in each category and total daily scores were averaged. Data represent the means and standard errors for 5-7 mice and are representative of two independent experiments. Survival curves were compared using log-rank Mantel-Cox curve comparison. Weight loss and clinical score data were compared using multiple student's *t* tests with Holm-Sidak multiple comparison correction. Significant differences compared to Mock/PR8 are indicated *P < 0.05, **P < 0.01, *** P < 0.001.

FIG 2 PR8 titers in the lungs of mice infected by PR8 or co-infected by RV two days before PR8. Mice were either mock-inoculated or inoculated with $7.6x10^6$ $TCID_{50}$ units of RV on day -2. On day 0, mice were either mock-inoculated or inoculated with ~100 $TCID_{50}$ units of PR8. PR8 was titrated by $TCID_{50}$ assay of homogenized lungs. Data for individual mice are shown with lines indicating means and standard errors for each group. The dotted line indicates the limit of detection of the assay. Titers were compared between groups using a student's *t*-test, which determined they were not significantly different.

FIG 3 Immunohistochemistry of PR8 antigen in the lungs of mice infected by PR8 or co-infected with RV two days before PR8. Images taken in the indicated regions of the lungs and at the indicated magnifications show (A) mice given mock inoculations on days -2 and 0 and (B, C) mice given Mock/PR8 or RV/PR8 on day -2/day 0. Tissue sections were immunostained for the PR8 hemagglutinin protein, which was visualized by vector red, and counterstained with hematoxylin. Lung tissues were collected on (B) day 4 and (C) day 7 after PR8 inoculation. Images were representative of multiple sections from two animals per group and time point. Arrows show examples of antigen in epithelial cells; arrowheads show examples of antigen in leukocytes, predominantly macrophages and neutrophils; stars indicate mucopurulent material.

FIG 4 Growth curves of PR8 from cells infected by PR8 or RV and PR8. LA-4 cells were inoculated with RV (moi = 1) (A) simultaneously with, (B) 6 hours before, or (C) 12 hours before inoculation with PR8 (moi =1). Media was collected at the indicated times after PR8

718 inoculation and titrated for PR8 by $TCID_{50}$ assay. Significant differences compared to Mock/PR8
719 were determined by students *t*-test. *P < 0.05, **P < 0.01, *** P < 0.001.

720

721 **FIG 5** Histopathology of mouse lungs infected by PR8 or co-infected with RV two days before
722 PR8. Mice were either mock-inoculated or inoculated with $7.6x10^6$ $TCID_{50}$ units of RV on day -
723 2. On day 0, mice were either mock-inoculated or inoculated with ~100 $TCID_{50}$ units of PR8.
724 Lungs were paraffin-embedded and sections were stained with hematoxylin and eosin. Images
725 were representative of multiple tissue sections from two mice per group and time point. (A)
726 shows images from lung sections of Mock/Mock inoculated mice taken with 10X and 40X
727 objectives. (B) shows images from the indicated groups and days taken with 10X objective. (C)
728 shows images from the indicated groups and days taken with 40X objective. Labeled structures
729 include bronchioles (B), terminal bronchioles (T), respiratory bronchioles (R), normal alveoli
730 (An), inflamed alveoli (Ai), and blood vessels (V).

731

732 **FIG 6** Disease kinetics in mice co-infected by RV two days before, simultaneously with, or two
733 days after PR8. Groups of 6-7 BALB/c mice were either mock-inoculated or inoculated with
734 $7.6x10^6$ $TCID_{50}$ units of RV two days before (RV/PR8), simultaneously with (RV+PR8), or two
735 days after (PR8/RV) either inoculation with ~100 ($PR8_{Low}$) or ~200 ($PR8_{Med}$) $TCID_{50}$ units of
736 PR8. Mice were monitored for mortality, weight loss, and clinical signs of disease (lethargy,
737 ruffled fur, hunched posture, labored breathing) for 14 days after PR8 inoculation. (A-C) RV and
738 low dose PR8 co-infection mortality (A), weight loss (B), and clinical scores (C). (D-F) RV and
739 medium dose PR8 co-infection mortality (D), weight loss (E), and clinical scores (F). Survival

curves were compared using log-rank Mantel-Cox curve comparison. Weight loss and clinical score data were compared using multiple student's *t* tests with Holm-Sidak multiple comparison correction. Significant differences compared to Mock/PR8 are indicated *P < 0.05, **P < 0.01, *** P < 0.001.

FIG 7 Disease kinetics in mice co-infected by MHV two days before PR8. Groups of 5-6 BALB/c mice were either mock-inoculated or inoculated with $2.0x10^3$ (MHV_{2000}), $1.0x10^3$ (MHV_{1000}), or $2.0x10^2$ (MHV_{200}) PFU of MHV two days before inoculation with ~100 $TCID_{50}$ units of PR8. Mice were monitored for mortality, weight loss, and clinical signs of disease (lethargy, ruffled fur, hunched posture, labored breathing) for 14 days after PR8 inoculation. (A-C) MHV_{2000} and PR8 co-infection mortality (A), weight loss (B), and clinical scores (C). (D-F) MHV_{1000} and PR8 co-infection mortality (D), weight loss (E), and clinical scores (F). (G-I) MHV_{200} and PR8 co-infection mortality (G), weight loss (H), and clinical scores (I). Survival curves were compared using log-rank Mantel-Cox curve comparison. Weight loss and clinical score data were compared using multiple student's *t* tests with Holm-Sidak multiple comparison correction. Significant differences compared to Mock/PR8 are indicated *P < 0.05, **P < 0.01, *** P < 0.001.

Figure 1

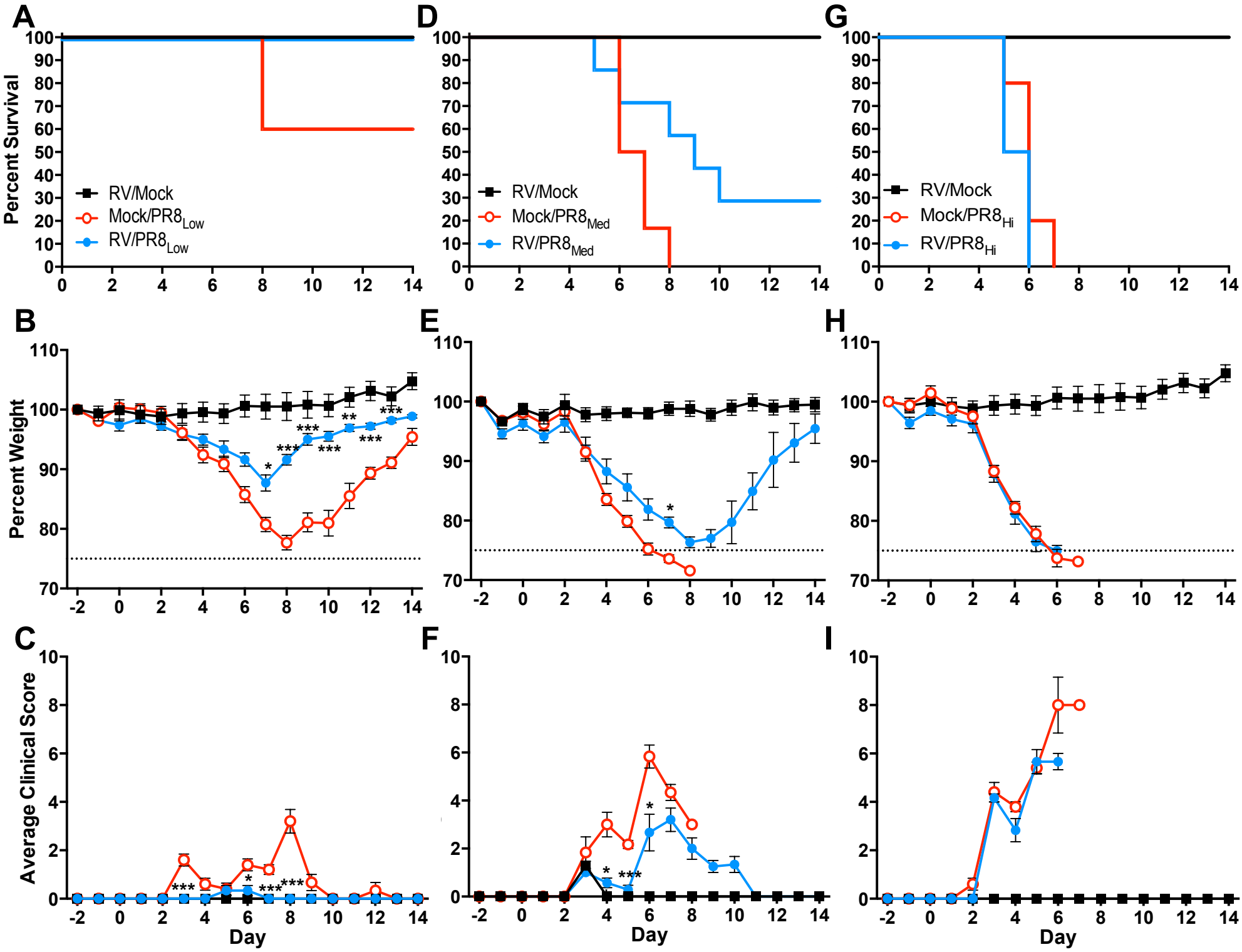
A
D
G
Percent Survival
RV/Mock
Mock/PR8Low
RV/PR8Low
Mock/PR8Med
RV/PR8Med
Mock/PR8Hi
RV/PR8Hi
B
E
H
Percent Weight
C
F
I
Average Clinical Score
Day

Figure 2

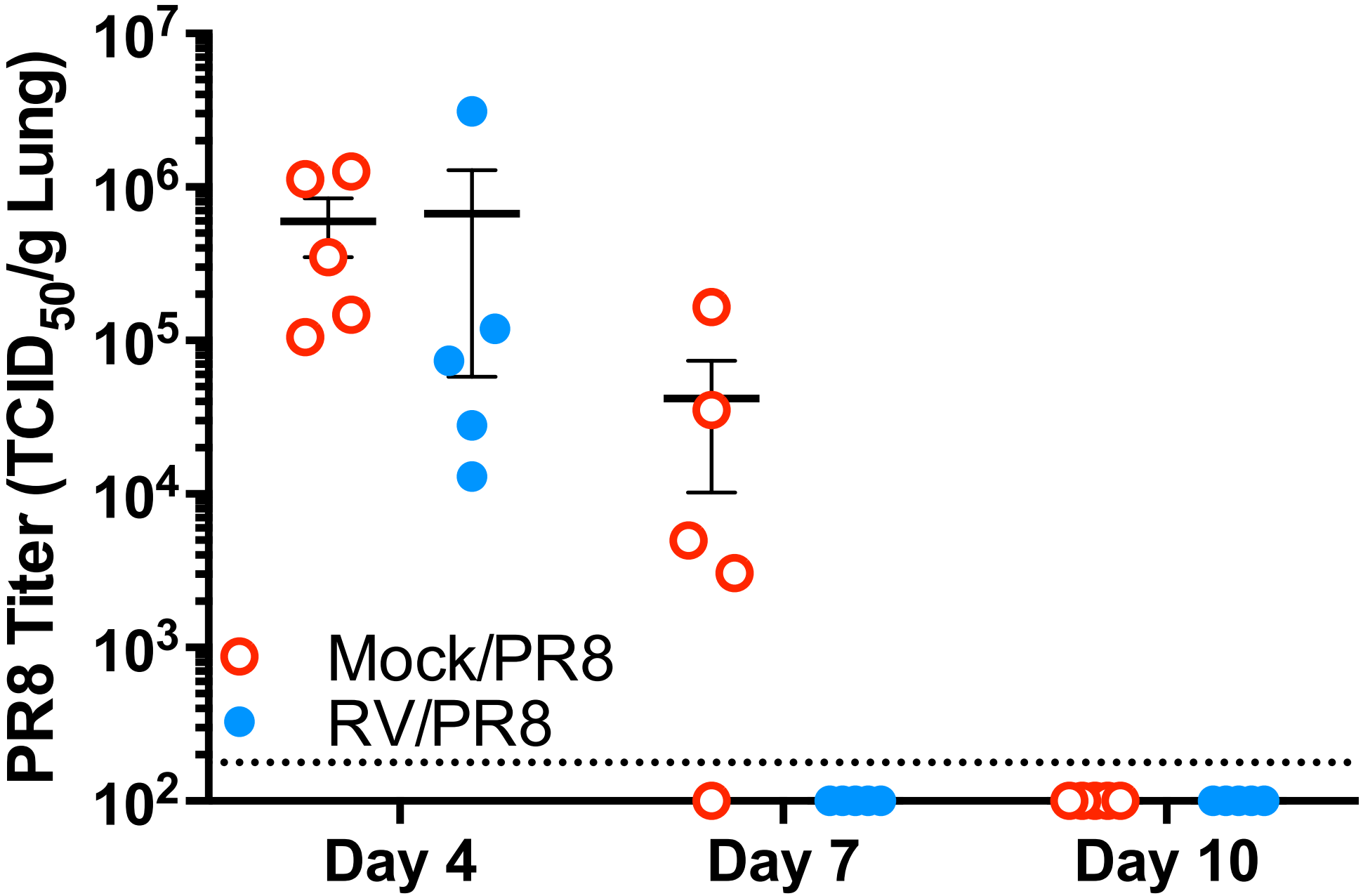
PR8 Titer (TCID50/g Lung)
10^7
10^6
10^5
10^4
10^3
10^2
Mock/PR8
RV/PR8
Day 4
Day 7
Day 10

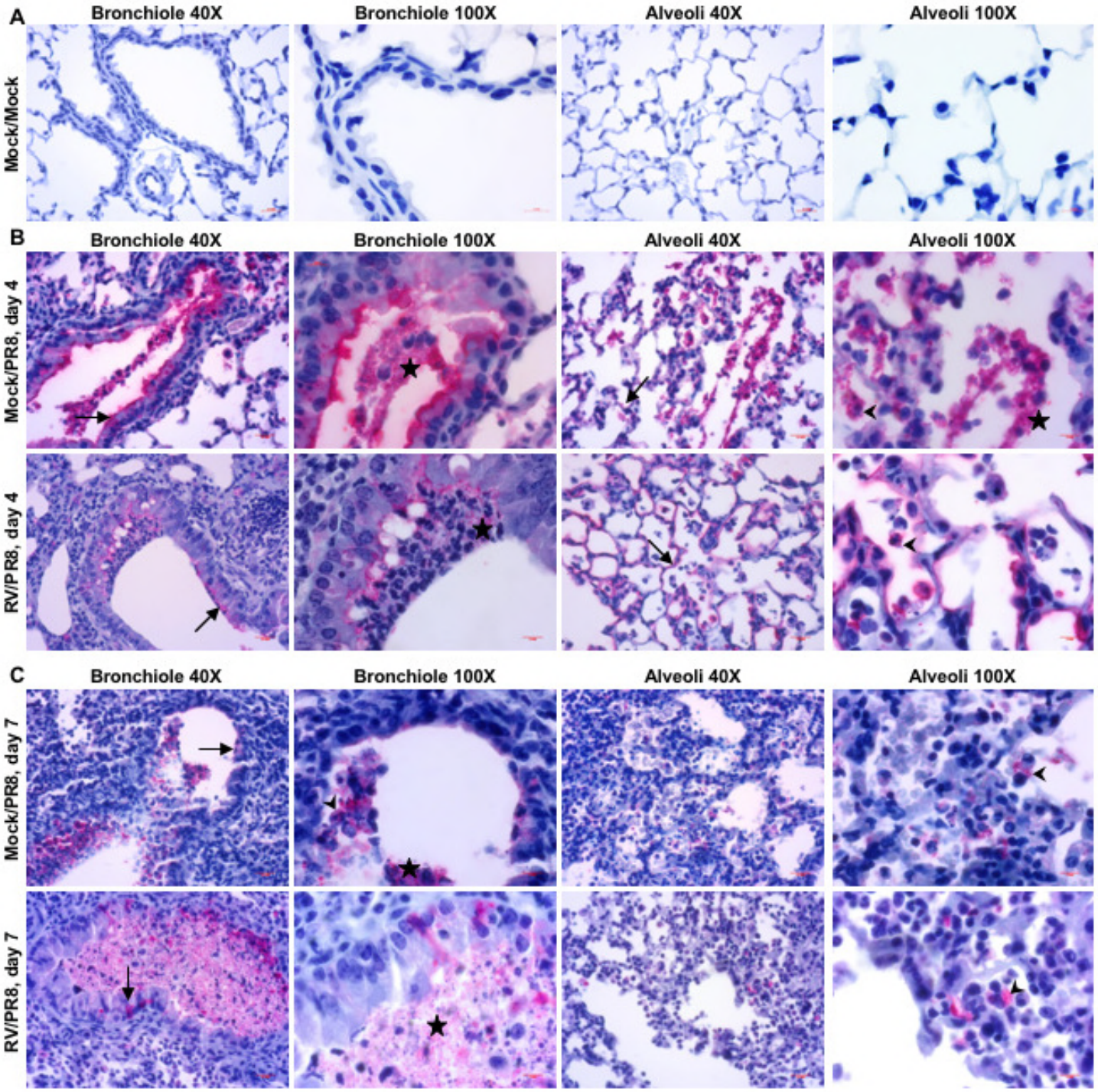

Figure 4

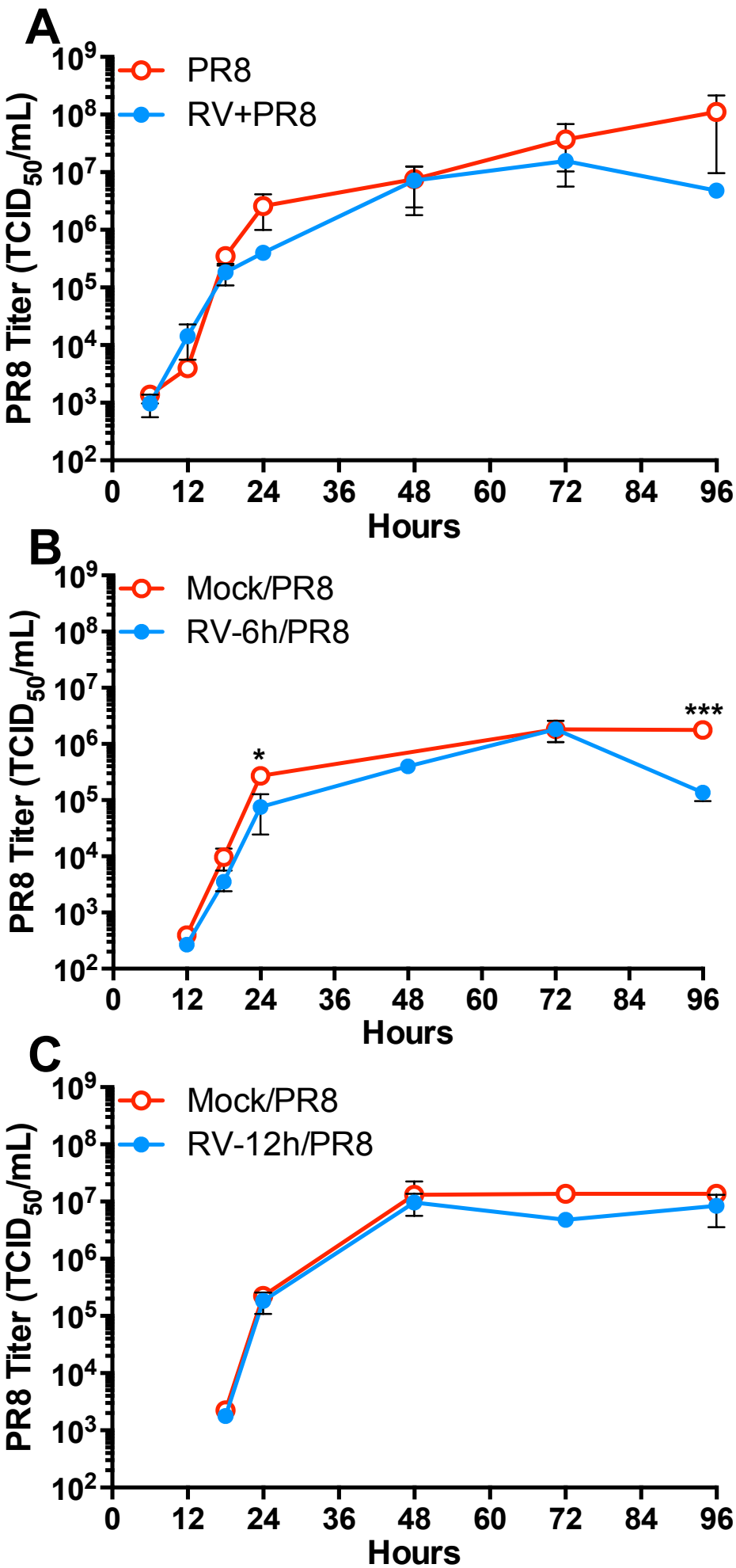

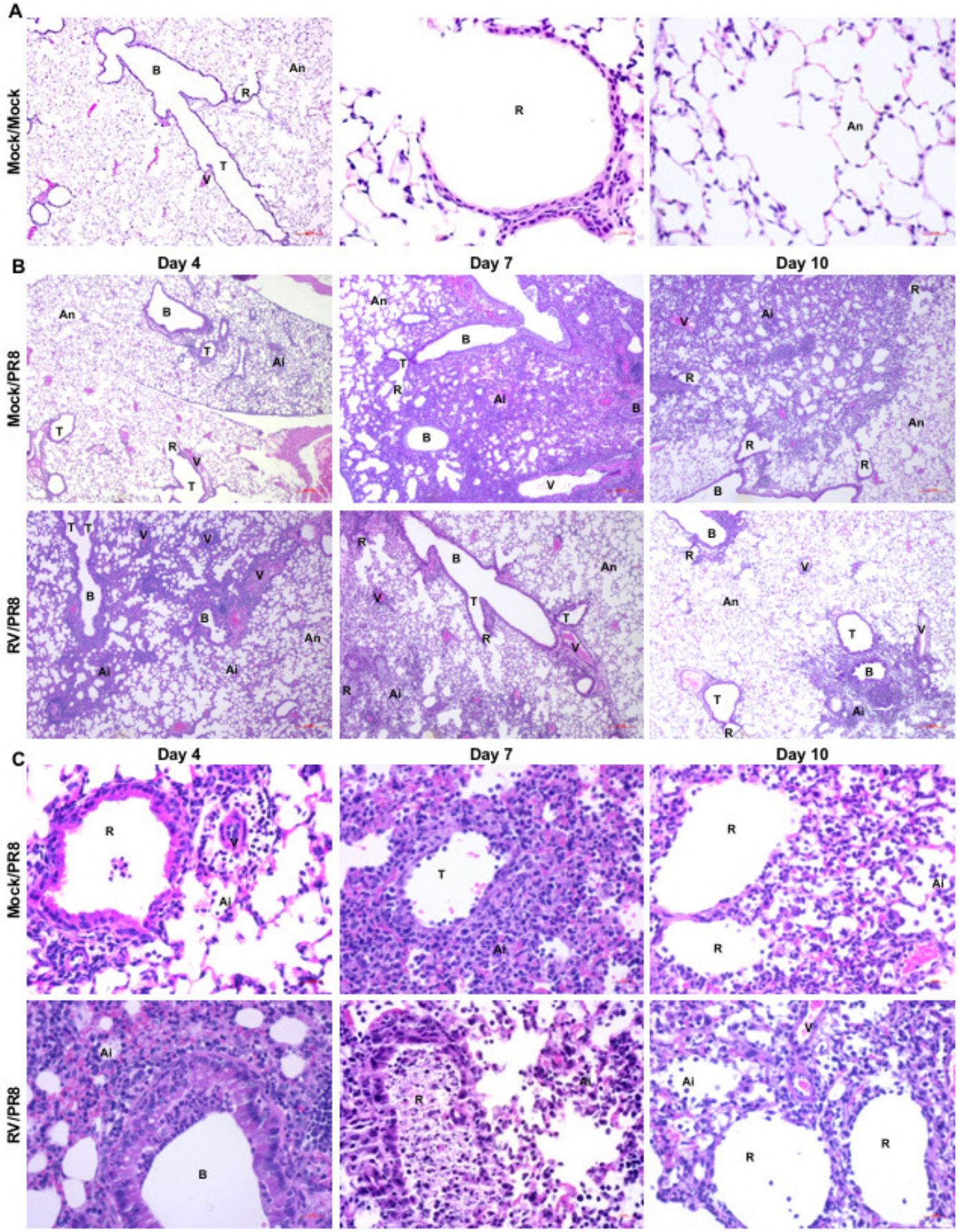

Figure 6

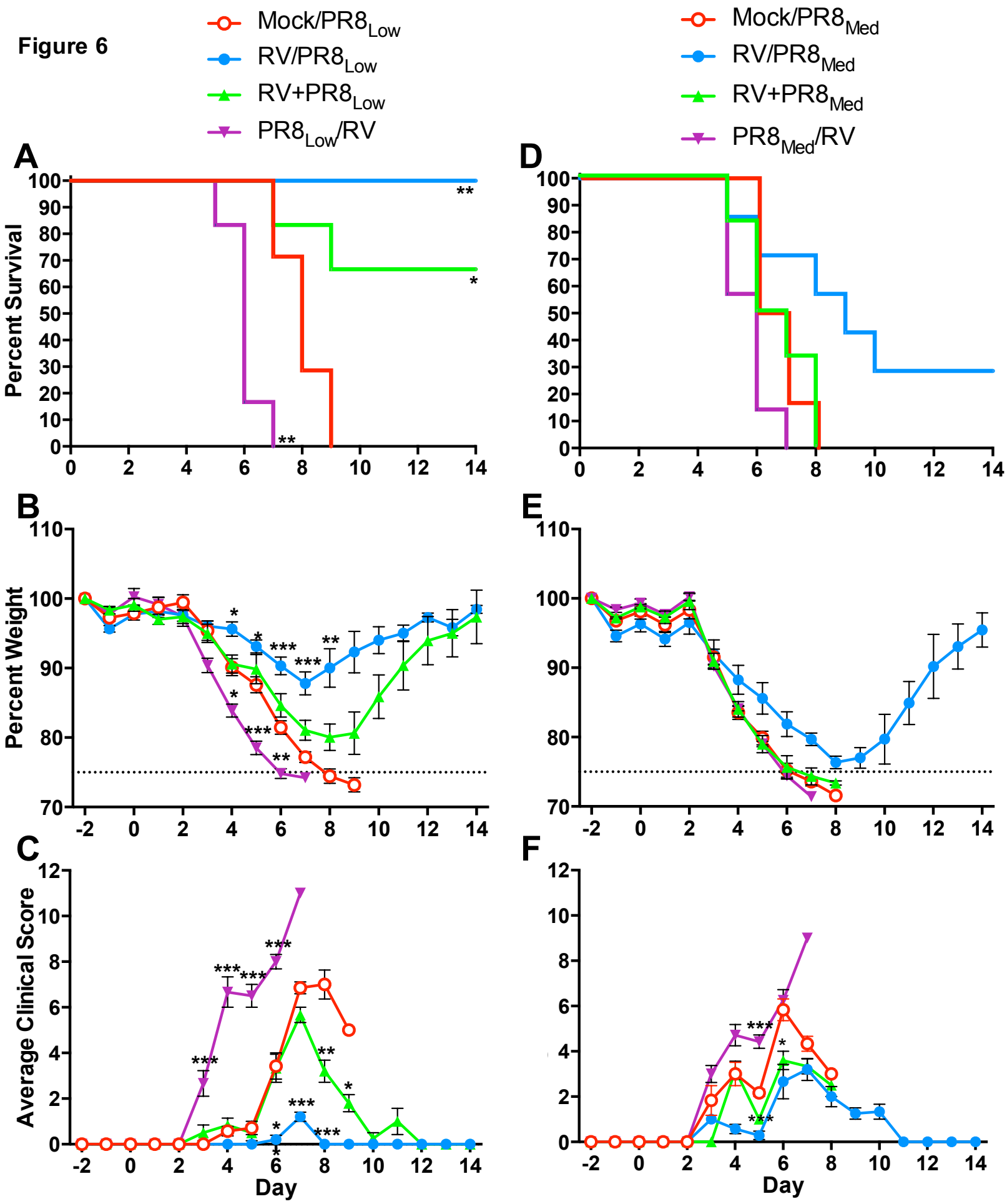

Figure 7

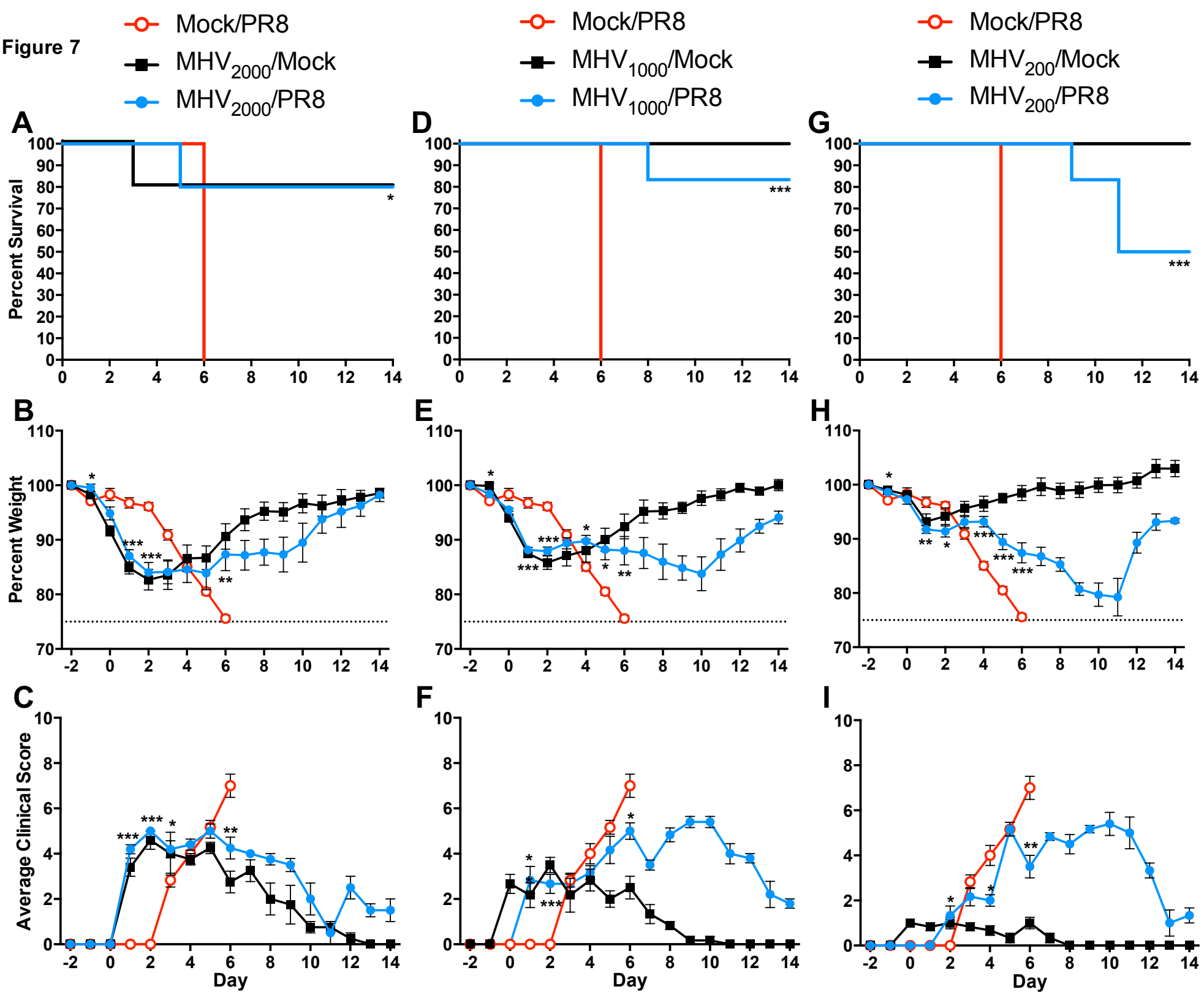
Mock/PR8
MHV2000/Mock
MHV2000/PR8
Mock/PR8
MHV1000/Mock
MHV1000/PR8
Mock/PR8
MHV200/Mock
MHV200/PR8
A
D
G
Percent Survival
B
E
H
Percent Weight
C
F
I
Average Clinical Score
Day
Day
Day